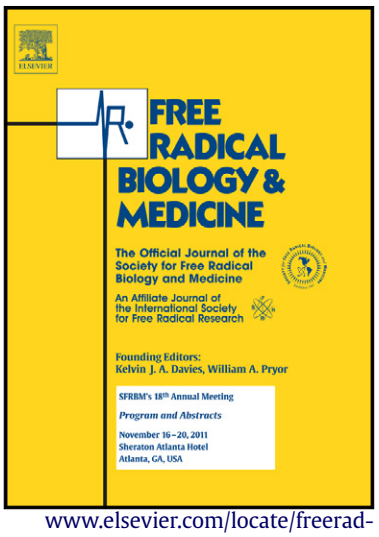

Proopiomelanocortin gene delivery induces apoptosis in melanoma through NADPH oxidase 4-mediated ROS generation

Guei-Sheung Liu, Jian-Ching Wu, Han-En Tsai, Gregory J. Dusting, Elsa C. Chan, Chieh-Shan Wu, Ming-Hong Tai

www.elsevier.com/locate/freerad-biomed

PII: S0891-5849(13)01565-7
DOI: http://dx.doi.org/10.1016/j.freeradbiomed.2013.12.024
Reference: FRB11857

To appear in: *Free Radical Biology and Medicine*

Cite this article as: Guei-Sheung Liu, Jian-Ching Wu, Han-En Tsai, Gregory J. Dusting, Elsa C. Chan, Chieh-Shan Wu, Ming-Hong Tai, Proopiomelanocortin gene delivery induces apoptosis in melanoma through NADPH oxidase 4-mediated ROS generation, *Free Radical Biology and Medicine,* http://dx.doi.org/10.1016/j.freeradbiomed.2013.12.024

Proopiomelanocortin gene delivery induces apoptosis in melanoma through NADPH oxidase 4-mediated ROS generation

Guei-Sheung Liu[a,b1], Jian-Ching Wu[c1], Han-En Tsai[d], Gregory J. Dusting[a,b], Elsa C. Chan[a,b], Chieh-Shan Wu[e], Ming-Hong Tai[c,d,f*]**

[a]Centre for Eye Research Australia, Victoria 3002, Australia

[b]Department of Ophthalmology, University of Melbourne, Victoria 3002, Australia

[c]Graduate Program in Marine Biotechnology, College of Marine Sciences, National Sun Yat-sen University, Kaohsiung 804, Taiwan

[d]Institute of Biomedical Science, National Sun Yat-sen University, Kaohsiung 804, Taiwan

[e]Department of Dermatology, Kaohsiung Veterans General Hospital, Kaohsiung 813, Taiwan

[f]Center for Neuroscience, National Sun Yat-sen University, Kaohsiung 804, Taiwan

[*]Corresponding author at: National Sun Yat-sen University, Institute of Biomedical Science, 70 Lien-Hai Road, Kaohsiung 804, Taiwan. Tel.: +88 67525 2000; fax: +88 675 250 197.

[**]Corresponding author. Tel.: +88 673 468 208; fax: +88 673 468 209.

Email: minghongtai@gmail.com

Email: rickliu0817@gmail.com

Abstract

Hypoxia in the tumor microenvironment triggers differential signaling pathways for tumor survival. In this study, we characterized the involvement of hypoxia and reactive oxygen species (ROS) generation in the anti-neoplastic mechanism of proopiomelanocortin (POMC) gene delivery in mouse B16-F10 melanoma model *in vivo* and *in vitro*. Histological analysis revealed increased TUNEL-positive cells and enhanced hypoxic activities in melanoma treated with adenovirus encoding POMC (Ad-POMC) but not control vector. Because the apoptotic cells were detected mainly in regions distant from blood vessels, it was hypothesized that POMC therapy might render melanoma cells vulnerable to hypoxic insults. Using a hypoxic chamber or cobalt chloride ($CoCl_2$), we showed that POMC gene delivery

[1] Both contributed equally to this work as first author.

elicited apoptosis and caspase-3 activation in cultured B16-F10 cells only in hypoxic conditions. The apoptosis induced by POMC gene delivery was associated with elevated ROS generation *in vitro* and *in vivo*. Blocking ROS generation using the antioxidant N-acetyl-L-cysteine abolished the apoptosis and caspase-3 activities induced by POMC gene delivery and hypoxia. We further showed that POMC-derived melanocortins, including α-MSH, β-MSH and ACTH, but not γ-MSH, contributed to POMC-induced apoptosis and ROS generation during hypoxia. To elucidate the source of ROS generation, application of the NADPH oxidase inhibitor, diphenyliodonium (DPI) attenuated α-MSH-induced apoptosis and ROS generation, implicating the pro-apoptotic role of NADPH oxidase in POMC action. Of the NADPH oxidase isoforms, only Nox4 was expressed in B16-F10 cells, and Nox4 was also elevated in Ad-POMC-treated melanoma tissues. Silencing Nox4 gene expression with Nox4 siRNA suppressed the stimulatory effect of α-MSH-induced ROS generation and cell apoptosis during hypoxia. In summary, we demonstrated that POMC gene delivery suppressed melanoma growth by inducing apoptosis, which was at least partly dependent on Nox4 upregulation.

Keywords

POMC, Melanoma, Apoptosis, ROS, NADPH oxidase

INTRODUCTION

Hypoxia plays a critical role in cancer development and progression. Low oxygen concentrations in the tumor microenvironment facilitate recruitment of vascular endothelial cells and promote angiogenesis to supply oxygen and nutrients to tumor cells. To adapt metabolically to hypoxic conditions, tumor cells also exhibit increased glucose transport and anaerobic glycolysis[1]. Fifty to sixty percent of locally advanced solid tumors, including melanomas, are characterized by areas of hypoxia/anoxia that result from an imbalance between oxygen supply and consumption in proliferating tumor cells. This imbalance is further exacerbated by a compromised tumor vasculature[2]. Studies have shown that presence of hypoxia within a tumor is an independent marker of a poor prognosis for patients with various cancer types including cutaneous melanomas[3].

Because stringent hypoxia/anoxia (<0.5% O_2) is toxic for normal and tumor cells, it can promote tumor progression by selecting cells with mutations that allow them to survive in these extreme conditions[4]. Furthermore, hypoxia activates signaling pathways that trigger neovascularization and that facilitates tumor cell invasion, migration, adhesion, and metastasis[5].

ROS are oxygen-containing, short-lived molecules that are highly reactive. The most common examples include superoxide, hydrogen peroxide (H_2O_2), hydroxyl radical (·OH), nitric oxide (NO) and peroxynitrite ($ONOO^-$). ROS are generally considered as unwanted by-products produced from aerobic metabolism, for instance superoxide is produced during mitochondrial oxidative phosphorylation[6]. Various enzyme systems produce ROS, including mitochondrial electron transport chain, cytochrome P450, lipooxygenase, cyclooxygenase, NADPH oxidase complex, xanthine oxidase and peroxisomes[7]. ROS are increased in malignant cells in part as a result of oncogene signaling via the NADPH oxidase complex and by hypoxia-related mitochondrial ROS. Increased oxidant levels contribute to enhanced cell proliferation and suppression of apoptosis. Oxygen depletion stimulates mitochondria to produced ROS[8], which activate signaling pathways involving hypoxia inducible factor 1α (HIF1α), that in turn promote cancer cell survival and tumor growth[9, 10]. However, an overproduction of ROS can cause apoptosis by opening the mitochondrial permeability transition pore and thus release proapoptotic factors[11, 12]. How cancer cells manage the balance of ROS during cancer development still remains unclear.

Pro-opiomelanocortin (POMC) is a stress hormone and is processed into various neuropeptides including adrenocorticotrophic hormone (ACTH), (α-, β-, γ- melanocyte-stimulating hormone [MSH]) and β-endorphin (β-EP) through the POMC-processing enzymes such as Prohormone convertases 1 and 2 (PC1/2). POMC-derived peptides possess pleiotropic functions, including pigmentation, adrenocortical function, regulation of energy homeostasis, and immunity modulation, in the central and peripheral systems[13-16]. POMC-derived peptide, α-MSH, has been reported to trigger melanoma and melanocyte differentiation[17] and potently inhibits migration and invasion of B16-BL6 melanoma cells *in vitro* and *in vivo*[18]. These findings suggest that POMC expression may inhibit the tumorigenicity of tumors.

We and others recently showed that targeted gene therapy with POMC suppressed growth of melanoma and lung cancer in animals[19-21]. In this study, we therefore characterized the tumor suppressive mechanisms of POMC in a mouse model of melanoma *in vivo* and *in vitro*, by overexpressing POMC using adenoviruses carrying POMC gene. We first characterized the effect of POMC overexpression on cell apoptosis and then explored how POMC overexpression caused apoptosis under hypoxia. We identified a novel tumor suppressive mechanism of POMC by facilitating cell apoptosis through modulation of the ROS-inducing enzyme NADPH oxidase 4 (Nox4) in melanoma. POMC gene delivery may represent novel therapeutic revenue for the treatment of melanoma.

MATERIALS AND METHODS

Preparation of adenovirus vectors- To overexpress POMC in B16-F10 melanoma cells, cells were infected with recombinant adenoviruses containing POMC genes (Ad-POMC) or control green fluorescent protein (Ad-GFP). Ad-GFP and Ad-POMC were generated as previously described [22].

Primary melanoma models and gene delivery- All animal experiments were carried out under protocols approved by Animal Care and Use Committee (IACUC) of National Sun Yet-Sen University. To induce the primary melanoma, B16-F10 cells were subcutaneously injected into C57BL/6 mice ($5x10^5$ cells in 0.1 ml of PBS; n=13-15) to monitor tumor growth. After tumors had grown to at least 100 mm^3 (10 days after implantation), mice were administered adenoviral vector at the indicated doses in 0.1 ml of PBS via intratumor injection. Subsequently, tumor volumes were measured with a dial-caliper according to the following formula: $width^2$ x length x 0.52. For tumor-suppressing studies, experiments were terminated when the tumor burden exceeded 10% of the animal's normal body weight.

Terminal deoxynucleotidyl transferase (TdT) mediated dUTP nick end labelling (TUNEL) assay- B16-F10 melanoma cells were implanted at day 0 and treated with intravenous injection of adenovirus vectors at day 10. After treatment for 21 days, cell death in frozen mouse melanoma sections was detected by enzyme labelling of DNA strand breaks using a TUNEL assay (*In Situ* Cell Death Detection Kit; Roche, Germany) according to manufacturer's instructions. Briefly, sections were incubated with a mixture of terminal

transferase (TdT) and fluorescein-dUTP reaction at 37 ℃ to label free 3'OH ends of genomic DNA. After TUNEL staining, sections were counterstained with propidium iodide (PI; 500 ng/ml) for 30 min at 25 ℃ and viewed under a fluorescent microscope. For quantifying the immunostaining of TUNEL, each sample was randomly captured by microscopy for at least five independent fields. An apoptotic index was estimated by normalizing the number of TUNEL positive cells to the total number of PI positive cells and calculated from five independent fields with a 40x microscopic field.

***In situ* detection of hypoxia**- Cells undergoing hypoxia and apoptosis in mouse tumor tissue sections were detected using pimonidazole (Hypoxyprobe-1, Burlington, MA, USA) and TUNEL kit according to manufacturers's instructions. Sections were then countered stained with DAPI.

Cell cultures and reagents- Mouse (B16-F10) and human (A375 and A2058) melanoma cells, mouse fibroblast cells (NIH3T3) and rat hepatocytes (clone 9) were purchased from ATCC (Manassas, VA) and cultured and maintained in complete medium made up of DMEM (Invitrogen; Carlsbad, CA) with 10% fetal bovine serum (FBS; Hyclone, USA), 2 mM glutamine, 100 mg/ml streptomycin (Invitrogen; Carlsbad, CA) and 100 U/ml penicillin, at 37 ℃ in 5% CO_2 atmosphere. ACTH, α-MSH, β-MSH and γ-MSH were purchased from BACHEM (Torrance, CA). $CoCl_2$, diphenyleneiodonium chloride (DPI), rotenone, allopurinol, 2,7-dichlorodihydrofluorescein diacetate (DCFH-DA), dihydroethidium (DHE), N-acetyl-L-cysteine (NAC) and indomethacin were purchased from Sigma-Aldrich (St. Louis, MO, USA).

Treatment of hypoxia- To mimic hypoxic condition, cells were incubated in commercially available hypoxia system (< 1% of oxygen), GENbox Jar (BioMerieux), was used as previously described[23] or treated with a pharmacological agent cobalt chloride ($CoCl_2$, 100 μM) at 37 ℃. The duration of hypoxia treatment is between 48 and 72 h depending on experimental conditions as described below.

Cell cycle analysis- B16-F10 cells were infected with Ad-POMC and Ad-GFP at a MOI of 1000 for 48 h. Following infections, cells were maintained in complete medium with reduced FBS (1 %) for hypoxia treatments. Cells were harvested, washed twice with PBS prior to fixation with ice-cold ethanol (70%) and then stored overnight at -20 ℃. Cells were washed twice with PBS prior to incubation with RNase A (10 μg/ml) and PI (50 μg/ml) for

30 min at 37 °C. DNA content of 20000 events was analyzed using a FACS Caliber flow cytometer (Becton Dickinson Biosciences; San Jose, CA) and CELLQuest software.

Measurement of ROS generation by DCFDA- Intracellular ROS concentration was measured using 2', 7'-dichlorofluoresceindiacetate (DCFDA) as previously described[24]. For gene delivery, cells (1×10^5 cells/well) were seeded in 6-well plates and subjected to infection with adenovirus vectors at a MOI of 1000 for 24 h and hypoxia treatments for another 24 h prior to DCFDA. For peptide treatment, B16-F10 cells (1×10^5 cells/well) were seeded in 6-well plates and pre-treated with ACTH, α-MSH, β-MSH and γ-MSH (10 nM) for 24 h and then incubated with $CoCl_2$ (100 μM) for another 24 h prior to DCFDA. Cells were rinsed with HBSS (Hanks balanced salt solution), loaded with DCFDA (10 μM), and incubated for 15 min at 37 °C. DCF fluorescent signals were detected immediately by FACS Caliber flow cytometer (Becton Dickinson Biosciences; San Jose, CA) and CELLQuest software.

Hydrogen peroxide (H_2O_2) measurement by Amplex red- Extracellular H_2O_2 was detected using Amplex red assay as previously described[24]. For gene delivery, cells (1×10^5 cells/well) were seeded in 6-well plates and subjected to infection with adenovirus vectors at a MOI of 1000 for 24 h and hypoxia treatments for another 24 h prior to Amplex red assay. For peptide treatment, cells (1×10^5 cells/well) were seeded in 6-well plates and pre-treated with ACTH, α-MSH, β-MSH and γ-MSH (10 nM) for 24 and then incubated with $CoCl_2$ (100 μM) for another 24 h prior to Amplex red assay. After treatments, cells were suspended in Krebs-Hepes buffer (HBSS, 98 mM NaCl, 4.7 mM KCl, 25 mM $NaHCO_3$, 1.2 mM $MgSO_4$, 1.2 mM KH_2PO_4, 2.5 mM $CaCl_2$, 11.1 mM D-glucose, and 20 mM Hepes-Na) containing Amplex red reagent (Invitrogen). Fluorescence was then measured with excitation and emission at 480 and 530 nm, respectively, using a Polarstar microplate reader (BMG Labtech) at 37 °C.

***In situ* superoxide detection**- The superoxide in frozen tumor section was detected by DHE (5 μM) as previously described[25]. Briefly, after TUNEL staining, the sections were incubated with DHE for 30 min at 37 °C in a humidified chamber protected from light. The red fluorescence was detected using a fluorescent microscope (DP70, Olympus, Japan).

Caspase-3 activity assay- Caspase-3 activity was measured by CaspACE Assay System, Colorimetric kit (Promega, Madison, WI). Briefly, cells (2 ×10^5 cells/well) were seeded in a 6-well tissue culture plate (Falcon, England). After an infection with adenovirus vectors at a MOI of 1000 for 24 h, cells were incubated with $CoCl_2$ (100 μM) and absence or presence NAC (10mM) in 1% FBS medium for 24 h. The lysate (100 μg) was added to the CaspACE assay buffer containing the caspase-3 substrate Ac-DEVD-p-nitroaniline (Ac-DEVD-pNA) and incubated for 4 h at 37 ℃. Cells treated with DMSO were used as controls. Absorbance at 405 nm was reading by a scanning multi-well spectrophotometer (Dynatech Laboratories, Chantilly, VA).

Western blot- Cell lysates were prepared and protein expression was measured as previously described[22]. The PVD membrane was blocked with 5 % milk in TBS-T for 1 h then incubated with specific primary antibodies against Nox4 (1:500 dilutions; Santa Cruz Inc; Santa Cruz, CA, USA) and β-actin antibodies (1:10000 dilutions; Sigma; St. Louis, MO, USA) for 1 h at room temperature. After incubation with secondary antibody conjugated with HRP (1:10000 dilutions in 5 % milk) for 1 h, signals on membrane were detected using chemiluminescent HRP substrate (Millipore Corporation; Billerica, MA, USA) and exposed to X-ray film for autoradiogram.

Quantitative real-time PCR- RNA was isolated from B16-F10 cells using RNAzol according to manufacturer's instructions (TEL-TEST, Inc., Friendswoods, TX, USA). Two μg of total RNA was used for reverse transcription with Superscript III (Invitrogen) using olio-dT and random primers. For quantitative real-time PCR, reactions were performed in an ABI Prism 7700 system (Applied Biosystems, Foster City, CA, USA) using the SYBR Green PCR master mix and the predesigned gene-specific probe and primer sets for mouse Nox4 (NM_015760.4). Data were normalized to β-actin (NM_007393.3) and expressed as fold changes over that in the control experiments. The primer sequences were as follows: Nox4 forward primer (5 -CTC AAC TGC AGC CTC ATC CTT-3) and reverse primer (5 -ACT GAA AAG TTG AGG GCA TTC AC-3); β-actin forward primer (5 -GGA ATC CTG TGG CAT CCA T-3) and reverse primer (5 - GCT CAG GAG GAG CAA TGA T -3).

RNA interference- To knock down the gene expression of Nox4 we purchased the small interfering RNA (siRNA) from Santa Cruz Biochemistry, Inc. Cells were transfected for 4 h

and then incubated with complete medium for 48 h. After transfection, cells were then pretreated with $CoCl_2$ for 1 h prior to treat with and without α-MSH (10 nM) for 24 h before cell harvest.

Statistical analysis- Data are presented as mean 6 standard error of the mean (SEM). The mean data were analyzed with one-way analysis of variance (one-way ANOVA) followed by Newman-Keuls post hoc or t-test (for multiple comparisons). A P value of less than 0.05 was regarded as statistically significant.

RESULTS

POMC gene delivery induces apoptosis in melanoma

To evaluate the therapeutic potential of POMC gene delivery, mice bearing established melanoma were administered adenoviral vector and then monitored for tumor progression. Mice treated with Ad-POMC showed significantly retarded melanoma growth compared with those in control animals (Supplementary Fig. 1). To investigate the mechanism of POMC gene delivery on inhibition of tumor growth, tumor tissues were collected and subject to histological analysis. Fluorescent images in Fig. 1A demonstrated an accumulation of TUNEL-positive cells in tumor nodules surrounding blood vessels in Ad-POMC-infected tumors whereas little apoptotic cells were found in Ad-GFP-infected melanoma. Quantification analysis of apoptotic events confirmed that the apoptotic index in Ad-POMC-infected melanoma was significantly higher than that in Ad-GFP infected tumors (Fig. 1B).

POMC gene delivery induced apoptosis in melanoma cell under a hypoxic challenge

Since TUNEL positive apoptotic cells were detected predominantly in the ischemic region distant from blood vessels, POMC gene therapy appears to render melanoma cells susceptible to hypoxic challenge. To address this aim, the extent of hypoxia in tumor sections was detected with immunofluorescent microscopy using a conventional hypoxyprobe-1 kit. Ad-POMC infected tumor sections demonstrated a greater degree of hypoxia in comparison to Ad-GFP infected tissues (Fig. 1C). To examine whether cells undergoing apoptosis correlates with tissue hypoxia, tumor sections were co-stained with TUNEL and hypoxyprobe-1 probe. It was found that ischemic activity was localized in close

proximity to TUNEL-positive cells in Ad-POMC-infected tumors. Although there was little hypoxic and TUNEL positive signals in Ad-GFP tumors, the distribution patterns of both signals were similar to Ad-POMC infected tumors, suggesting that induction of apoptosis tends to occur in hypoxic regions.

Having established that the induction on cell apoptosis by systemic POMC gene delivery was associated with tissue hypoxia, we explored the mechanism underling such process in B16-F10 melanoma cells. We used a hypoxia chamber (<1% of oxygen) and a pharmacological agent $CoCl_2$ (100 μM) to mimic hypoxic conditions. Flow cytometry analysis demonstrated that the proportion of apoptotic cell was increased about 12% in Ad-POMC infected group in a hypoxia chamber (Fig. 2A). Cells treated with $CoCl_2$ analysed by flow cytometry analysis also showed an increase in apoptotic cells in Ad-POMC group when compared to Ad-GFP group (Fig. 2B). The stimulatory effect of POMC gene delivery on apoptosis in B16-F10 cells was further confirmed by evaluating the Caspase 3 activity. As shown in Fig. 2C, Ad-POMC induced an increase in caspase-3 activity in $CoCl_2$-induced hypoxia. Taken together, these results suggested that POMC gene delivery triggers melanoma cells toward program cell death under hypoxic challenges.

Melanocortins promoted apoptosis of melanoma cells under hypoxia

Our previous study demonstrated that POMC-derived peptides (α-MSH, β-MSH and ACTH) reduced colony formation and invasive potential in B16-F10 melanoma cells[19]. In this study, we characterize which POMC-derived peptides induced apoptosis in B16-F10 melanoma cells. To address this aim, cells were treated with 10 nM of α-MSH, β-MSH, ACTH and γ-MSH in $CoCl_2$-induced hypoxic condition. In flow cytometry analysis, α-MSH, β-MSH and ACTH peptides enhanced G0/G1 phase population through a reduction in cell numbers in S and M phases in normoxia, indicating cell cycle arrest (Supplementary Table 1). However, under hypoxia condition, α-MSH, β-MSH and ACTH peptides remarkably induced about 12% population of apoptotic cells in pre-G0 phase, whereas γ-MSH had no such effect (Fig 3). Similar effect was observed in two human melanoma cell lines (A375 and A2058), but not in two non-transformed cell lines (NIH3T3 and Clone 9) (Supplementary Fig. 2).

Therefore, we identified that α-MSH, β-MSH and ACTH but not γ-MSH induced apoptosis in melanoma cells during hypoxia and which is selectivity on melanoma cells.

Excessive ROS generation participated in POMC-induced apoptosis during hypoxia

Having established that POMC overexpression potentiated the effect of hypoxia on apoptosis of melanoma cells, we investigated the molecular mechanisms underlying such process. ROS have been implicated in the regulation of apoptosis in melanoma cells[26, 27]. We therefore performed *in-situ* detection of superoxide with DHE and TUNEL assay to assess the distribution of ROS production and cell apoptosis in Ad-POMC and Ad-GFP treated melanoma tissues. There was an accumulation of DHE fluorescence distant from blood vessel to far tumor region and such signal was co-localized with TUNEL-positive staining cells in Ad-POMC treated group (Fig. 4A). Little DHE fluorescence was detected in Ad-GFP treated melanoma tissues, suggesting that ROS generation is associated with cell apoptosis in melanoma (Fig. 4A). To elucidate a role of ROS generation in POMC-mediated cell apoptosis under hypoxia, we first examined the effect of POMC overexpression on ROS generation in B16-F10 melanoma cells under normal and $CoCl_2$-induced hypoxic conditions. Hypoxia increased total ROS production detected by DCF-DA in control and Ad-GFP infected cells, which was potentiated by an overexpression of POMC in melanoma cells infected with Ad-POMC (Fig. 4B). There was a tendency of increased H_2O_2 generation in hypoxic cells and such increase was potentiated by Ad-POMC treatment (Fig. 4C). Moreover, inhibition of ROS production with an antioxidant *N*-acetyl-$_L$-cysteine (NAC, 10 mM) was found to abrogate the Ad-POMC-stimulated augmentation of caspase-3 activity and also rescued the Ad-POMC induced apoptosis comparison with Ad-GFP group during hypoxia (Fig. 4D and 4E), indicating that ROS production contributed to Ad-POMC-induced apoptosis. In summary, our results suggested that ROS production by POMC gene delivery was involved in apoptosis in melanoma cells during hypoxia.

Melanocortins increased ROS generation in melanoma cells during hypoxia

We next examined which of the POMC-derived peptides elevated ROS generation in melanoma cells during hypoxia. To address this question, cells were treated with one of the

POMC-derived peptides, α-, β-, γ-MSH and ACTH (10 nM) for 24 h, then incubated with $CoCl_2$ (100 μM) for another 24 h before assessment of ROS production with DCFDA and amplex red assays. As shown in Fig 5A, $CoCl_2$-induced hypoxia stimulated DCFDA signals in melanoma cells and such induction was significantly potentiated by α-MSH, β-MSH and ACTH but not γ-MSH. H_2O_2 generation was also augmented by α-MSH, β-MSH and ACTH peptides in $CoCl_2$ group (Fig. 5B). Our results suggested that POMC-derived peptides (α-MSH, β-MSH and ACTH) contributed to ROS generation in melanoma during hypoxia.

ROS generation was mediated though α-MSH-induced Nox4 NADPH oxidase upregulation

α-MSH was found to modulate the inhibitory effect of systemic POMC delivery on the progression of melanoma[19]. We therefore used α-MSH peptide to investigate the source of ROS generation in cell apoptosis during hypoxia. Several endogenous enzymes including xanthine oxidase[28], mitochondria[29], cyclooxygenase[30] and NADPH oxidase[31] have been implicated as sources of ROS generation in melanoma cells. To investigate which enzyme sources were involved in α-MSH-mediated ROS generation during hypoxia, cells were treated with pharmacological inhibitor of these enzymes 10 min prior to Amplex red assay (Fig. 5C). None of the inhibitors affected basal H_2O_2 generation. Inhibitor of NADPH oxidase DPI (0.1 μM) significantly abrogated α-MSH-induced ROS generation during hypoxia. In contrast, inhibitor of xanthine oxidase (allopurinol, 50 μM) and cyclooxygenase (indomethacin, 1 μM) did not affect the stimulatory effect of α-MSH on H_2O_2 production, suggesting NADPH oxidase was a major source of α-MSH-mediated ROS generation in melanoma cells. We further investigated which of NADPH oxidase isoforms was involved in α-MSH-induced ROS production. By using quantitative PCR and western blot analysis of NADPH oxidase isoforms (Nox1 to Nox4), we first characterized the Nox4 expression in B16-F10 melanoma cells (Supplementary Fig. 3). Moreover, α-MSH enhanced Nox4 the mRNA and protein levels of Nox4 while other NADPH oxidase isoforms (Nox1, Nox2 and Nox3) remained undetected. Interestingly, α-MSH reversed the inhibitory effect of hypoxia on Nox4 expression (Fig. 5D and E), suggesting that the stimulatory effect of α-MSH eon

ROS generation in hypoxic condition was associated with an upregulation of Nox4 expression.

Silencing Nox4 gene expression rescued α-MSH-induced apoptosis during hypoxia

To investigate the role of Nox4 in α-MSH-induced apoptosis during hypoxia, gene silencing of Nox4 with siRNA was performed in B16-F10 melanoma cells. We first verified that transfection of Nox4 siRNA but not control siRNA significantly attenuated the mRNA and protein expression of Nox4 (Fig. 6A). Nox4 siRNA also remarkably abolished the intracellular and extracellular H_2O_2 generation compared and inhibited the stimulatory effect of hypoxia on ROS generation (Fig. 6B). Importantly, silencing of Nox4 gene expression successfully alleviated α-MSH-induced apoptosis during hypoxia (Fig. 6C). Moreover, immunostaining analysis revealed that Nox4 staining has strong fluorescence intensity in Ad-POMC infected group and displayed a positive correlation with TUNEL staining compared to Ad-GFP infected group (data not show). In summary, these results indicated that ROS-derived from Nox4 is involved in tα-MSH-induced apoptosis in melanoma cells during hypoxia.

DISCUSSION

In this study we clarified how Nox4-mediated ROS generation was a key signaling pathway involved in cell apoptosis mediated by POMC gene delivery in melanoma during hypoxic insults. Our results provide further understanding of the tumor suppressive mechanisms of POMC for treatments for melanoma.

Tissue oxygenation is an important component of the tumor microenvironment and contributes to melanocyte transformation and melanoma development[32]. Hypoxic microenvironment is a widespread phenomenon in tumors, especially in solid tumor[2]. Our data showed that POMC gene delivery rendered melanoma cells more susceptible to hypoxia-induced damage. Several studies have shown that accumulation of ROS was a major regulator to restrain downstream PI3K/AKT signaling pathway and regressed the Bcl-2/Bax ratio in melanoma[33, 34]. Excess ROS generation can cause apoptosis by triggering opens of the mitochondrial permeability transition pore and release of

proapoptotic factors[11, 12]. Our data revealed that the overload of ROS generation was a main operator for POMC-induced apoptosis in melanoma cells during hypoxia. However whether other sources of extracellular ROS generation from infiltrating neutrophils or phagocytes are involved in apoptosis in tumor hypoxic regions requires further investigation.

Several sources of ROS including mitochondrial enzymes and NADPH oxidase have been reported in melanoma cells[27]. In a previous study the expression of NADPH oxidase components p22phox and NOX4 were required to transform and promote malignant growth in human malignant melanoma cells[31]. Yamaura *et al*. also demonstrated that NOX4-mediated ROS generation contributed to proliferation and transformation of the melanoma phenotype by regulating G2-M cell cycle progression[35]. Besides, suppression of NADPH oxidase activity by targeting subunits Rac1 and p47phox was found to promote melanogenic differentiation in B16 melanoma cells[36]. We recently demonstrated that NADPH oxidase isoform Nox4 was a major source of ROS generation upon α-MSH stimulation. Nox4 acts as a feedback mechanism to control melanogenic differentiation by suppressing MITF-mediated tyrosinase mRNA expression[24]. Here, our data showed that the POMC-induced apoptosis in hypoxic condition was mediated by an upregulation of Nox4. The POMC-derived peptide, α-MSH, was found to stimulate ROS generation during hypoxia and this contributes to induce apoptosis in POMC gene therapy in melanoma. Suppressing Nox4 expression by siRNA or scavenging ROS accumulation by NAC reduced apoptosis in POMC gene delivery or α-MSH treated melanoma cells, pinpointing the role of Nox4-derived ROS in POMC-induced cell apoptosis. However, the precise molecular mechanism of how Nox4-derived ROS induced apoptosis by POMC gene delivery in melanoma cells remained unclear.

The melanocortin 1 receptor (MC1R) is one of the melanocortin receptors that has been shown to have a high binding affinity for its ligand α-MSH, and MC1R is implicated in several physiological functions including pigmentation and inflammation[37]. In all of these regulatory signaling pathways it has been shown that secondary messenger cAMP triggered downstream effector molecules protein kinase A (PKA) and cAMP-responsive element binding (CREB) protein 1 transcription factor promote Microphthalmia-associated transcription factor (MITF) in melanogenic differentiation[38]. Our recent study also

demonstrated that upregulation of NOX4 and ROS generation occurred through MC1R/PKA/MITF pathway in melanoma cells[24]. In the present study, our data showed that POMC gene delivery triggered ROS production, possibly through α-MSH, β-MSH and ACTH peptides that have high binding affinity to MC1R. Therefore, POMC-derived peptides such as α-MSH, β-MSH and ACTH triggered Nox4-derived ROS is likely driven by MC1R/cAMP/PKA/MITF pathway. However, the precise molecular mechanisms still needs further evaluation.

In summary, we identified that Nox4-mediated ROS generation was a major cause of apoptosis induced by POMC derived peptides during hypoxic insults. These observations provide a better understanding at the molecular level of the hypoxic condition in tumor environment. While our results provide an understanding of tumor suppressive mechanisms of POMC in mouse B16-F10 melanoma cells, which may facilitate a novel therapy for melanoma control.

AUTHOR DISCLOSURE STATEMENT

The authors who have taken part in this study declared that they do not have anything to disclose regarding funding from industry or conflict of interest with respect to this manuscript.

ACKNOWLEDGEMENTS

This work was supported by grants from the National Science Council, Taiwan (NSC 100-2325-B-110-002-MY3), Kaohsiung Veterans General Hospital, Taiwan (MF-DLC 98029S4 and MF-DLC 99053S4), National Sun Yat-Sen University and the Ophthalmic Research Institute of Australia (ORIA). G.S.L. receives the Early Career Researcher fellowship (from University of Melbourne). G.J.D receives a Principal Research Fellowship from NHMRC. G.S.L. and E.C.C. are supported by The Ansell Ophthalmology Foundation. J.C.W is supported by Graduate Program in Marine Biotechnology. The Centre for Eye Research Australia receives Operational Infrastructure Support from the Victorian Government.

REFERENCES

[1] Michaylira, C. Z.; Nakagawa, H. Hypoxic microenvironment as a cradle for melanoma development and progression. *Cancer biology & therapy* **5:**476-479; 2006.

[2] Vaupel, P.; Mayer, A. Hypoxia in cancer: significance and impact on clinical outcome. *Cancer metastasis reviews* **26:**225-239; 2007.

[3] Lartigau, E.; Randrianarivelo, H.; Avril, M. F.; Margulis, A.; Spatz, A.; Eschwege, F.; Guichard, M. Intratumoral oxygen tension in metastatic melanoma. *Melanoma research* **7:**400-406; 1997.

[4] Graeber, T. G.; Osmanian, C.; Jacks, T.; Housman, D. E.; Koch, C. J.; Lowe, S. W.; Giaccia, A. J. Hypoxia-mediated selection of cells with diminished apoptotic potential in solid tumours. *Nature* **379:**88-91; 1996.

[5] Rofstad, E. K.; Danielsen, T. Hypoxia-induced angiogenesis and vascular endothelial growth factor secretion in human melanoma. *British journal of cancer* **77:**897-902; 1998.

[6] Finkel, T. Signal transduction by reactive oxygen species. *The Journal of cell biology* **194:**7-15; 2011.

[7] Fruehauf, J. P.; Meyskens, F. L., Jr. Reactive oxygen species: a breath of life or death? *Clinical cancer research : an official journal of the American Association for Cancer Research* **13:**789-794; 2007.

[8] Guzy, R. D.; Schumacker, P. T. Oxygen sensing by mitochondria at complex III: the paradox of increased reactive oxygen species during hypoxia. *Experimental physiology* **91:**807-819; 2006.

[9] Chandel, N. S.; Maltepe, E.; Goldwasser, E.; Mathieu, C. E.; Simon, M. C.; Schumacker, P. T. Mitochondrial reactive oxygen species trigger hypoxia-induced transcription. *Proceedings of the National Academy of Sciences of the United States of America* **95:**11715-11720; 1998.

[10] Galanis, A.; Pappa, A.; Giannakakis, A.; Lanitis, E.; Dangaj, D.; Sandaltzopoulos, R. Reactive oxygen species and HIF-1 signalling in cancer. *Cancer letters* **266:**12-20; 2008.

[11] Fleury, C.; Mignotte, B.; Vayssiere, J. L. Mitochondrial reactive oxygen species in cell death signaling. *Biochimie* **84:**131-141; 2002.

[12] Brenner, C.; Grimm, S. The permeability transition pore complex in cancer cell death. *Oncogene* **25:**4744-4756; 2006.

[13] Raffin-Sanson, M. L.; de Keyzer, Y.; Bertagna, X. Proopiomelanocortin, a polypeptide precursor with multiple functions: from physiology to pathological conditions. *European journal of endocrinology / European Federation of Endocrine Societies* **149:**79-90; 2003.

[14] Garfield, A. S.; Lam, D. D.; Marston, O. J.; Przydzial, M. J.; Heisler, L. K. Role of central melanocortin pathways in energy homeostasis. *Trends in endocrinology and metabolism: TEM* **20:**203-215; 2009.

[15] Hegadoren, K. M.; O'Donnell, T.; Lanius, R.; Coupland, N. J.; Lacaze-Masmonteil, N. The role of beta-endorphin in the pathophysiology of major depression. *Neuropeptides* **43:**341-353; 2009.

[16] Rousseau, K.; Kauser, S.; Pritchard, L. E.; Warhurst, A.; Oliver, R. L.; Slominski, A.; Wei, E. T.; Thody, A. J.; Tobin, D. J.; White, A. Proopiomelanocortin (POMC), the ACTH/melanocortin precursor, is secreted by human epidermal keratinocytes and

melanocytes and stimulates melanogenesis. *FASEB journal : official publication of the Federation of American Societies for Experimental Biology* **21:**1844-1856; 2007.
[17] Smalley, K.; Eisen, T. The involvement of p38 mitogen-activated protein kinase in the alpha-melanocyte stimulating hormone (alpha-MSH)-induced melanogenic and anti-proliferative effects in B16 murine melanoma cells. *FEBS letters* **476:**198-202; 2000.
[18] Murata, J.; Ayukawa, K.; Ogasawara, M.; Fujii, H.; Saiki, I. Alpha-melanocyte-stimulating hormone blocks invasion of reconstituted basement membrane (Matrigel) by murine B16 melanoma cells. *Invasion & metastasis* **17:**82-93; 1997.
[19] Liu, G. S.; Tsai, H. E.; Weng, W. T.; Liu, L. F.; Weng, C. H.; Chuang, M. R.; Lam, H. C.; Wu, C. S.; Tee, R.; Wen, Z. H.; Howng, S. L.; Tai, M. H. Systemic pro-opiomelanocortin expression induces melanogenic differentiation and inhibits tumor angiogenesis in established mouse melanoma. *Human gene therapy* **22:**325-335; 2011.
[20] Tsai, H. E.; Liu, G. S.; Kung, M. L.; Liu, L. F.; Wu, J. C.; Tang, C. H.; Huang, C. H.; Chen, S. C.; Lam, H. C.; Wu, C. S.; Tai, M. H. Downregulation of Hepatoma-Derived Growth Factor Contributes to Retarded Lung Metastasis via Inhibition of Epithelial-Mesenchymal Transition by Systemic POMC Gene Delivery in Melanoma. *Molecular cancer therapeutics*; 2013.
[21] Tsai, H. E.; Liu, L. F.; Dusting, G. J.; Weng, W. T.; Chen, S. C.; Kung, M. L.; Tee, R.; Liu, G. S.; Tai, M. H. Pro-opiomelanocortin gene delivery suppresses the growth of established Lewis lung carcinoma through a melanocortin-1 receptor-independent pathway. *The journal of gene medicine* **14:**44-53; 2012.
[22] Liu, G. S.; Liu, L. F.; Lin, C. J.; Tseng, J. C.; Chuang, M. J.; Lam, H. C.; Lee, J. K.; Yang, L. C.; Chan, J. H.; Howng, S. L.; Tai, M. H. Gene transfer of pro-opiomelanocortin prohormone suppressed the growth and metastasis of melanoma: involvement of alpha-melanocyte-stimulating hormone-mediated inhibition of the nuclear factor kappaB/cyclooxygenase-2 pathway. *Molecular pharmacology* **69:**440-451; 2006.
[23] Hsiao, S. T.; Lokmic, Z.; Peshavariya, H.; Abberton, K. M.; Dusting, G. J.; Lim, S. Y.; Dilley, R. J. Hypoxic conditioning enhances the angiogenic paracrine activity of human adipose-derived stem cells. *Stem cells and development* **22:**1614-1623; 2013.
[24] Liu, G. S.; Peshavariya, H.; Higuchi, M.; Brewer, A. C.; Chang, C. W.; Chan, E. C.; Dusting, G. J. Microphthalmia-associated transcription factor modulates expression of NADPH oxidase type 4: a negative regulator of melanogenesis. *Free radical biology & medicine* **52:**1835-1843; 2012.
[25] Zhang, P.; Li, W.; Li, L.; Wang, N.; Li, X.; Gao, M.; Zheng, J.; Lei, S.; Chen, X.; Lu, H.; Liu, Y. Treatment with edaravone attenuates ischemic brain injury and inhibits neurogenesis in the subventricular zone of adult rats after focal cerebral ischemia and reperfusion injury. *Neuroscience* **201:**297-306; 2012.
[26] Tochigi, M.; Inoue, T.; Suzuki-Karasaki, M.; Ochiai, T.; Ra, C.; Suzuki-Karasaki, Y. Hydrogen peroxide induces cell death in human TRAIL-resistant melanoma through intracellular superoxide generation. *International journal of oncology* **42:**863-872; 2013.
[27] Wittgen, H. G.; van Kempen, L. C. Reactive oxygen species in melanoma and its therapeutic implications. *Melanoma research* **17:**400-409; 2007.
[28] Valverde, P.; Manning, P.; McNeil, C. J.; Thody, A. J. Activation of tyrosinase reduces the cytotoxic effects of the superoxide anion in B16 mouse melanoma cells. *Pigment cell research / sponsored by the European Society for Pigment Cell Research and the International Pigment Cell Society* **9:**77-84; 1996.

[29] Barbi de Moura, M.; Vincent, G.; Fayewicz, S. L.; Bateman, N. W.; Hood, B. L.; Sun, M.; Suhan, J.; Duensing, S.; Yin, Y.; Sander, C.; Kirkwood, J. M.; Becker, D.; Conrads, T. P.; Van Houten, B.; Moschos, S. J. Mitochondrial respiration--an important therapeutic target in melanoma. *PloS one* **7:**e40690; 2012.

[30] Denkert, C.; Kobel, M.; Berger, S.; Siegert, A.; Leclere, A.; Trefzer, U.; Hauptmann, S. Expression of cyclooxygenase 2 in human malignant melanoma. *Cancer research* **61:**303-308; 2001.

[31] Brar, S. S.; Kennedy, T. P.; Sturrock, A. B.; Huecksteadt, T. P.; Quinn, M. T.; Whorton, A. R.; Hoidal, J. R. An NAD(P)H oxidase regulates growth and transcription in melanoma cells. *American journal of physiology. Cell physiology* **282:**C1212-1224; 2002.

[32] Bedogni, B.; Powell, M. B. Hypoxia, melanocytes and melanoma - survival and tumor development in the permissive microenvironment of the skin. *Pigment cell & melanoma research* **22:**166-174; 2009.

[33] Lee, J. H.; Won, Y. S.; Park, K. H.; Lee, M. K.; Tachibana, H.; Yamada, K.; Seo, K. I. Celastrol inhibits growth and induces apoptotic cell death in melanoma cells via the activation ROS-dependent mitochondrial pathway and the suppression of PI3K/AKT signaling. *Apoptosis : an international journal on programmed cell death* **17:**1275-1286; 2012.

[34] Mayola, E.; Gallerne, C.; Esposti, D. D.; Martel, C.; Pervaiz, S.; Larue, L.; Debuire, B.; Lemoine, A.; Brenner, C.; Lemaire, C. Withaferin A induces apoptosis in human melanoma cells through generation of reactive oxygen species and down-regulation of Bcl-2. *Apoptosis : an international journal on programmed cell death* **16:**1014-1027; 2011.

[35] Yamaura, M.; Mitsushita, J.; Furuta, S.; Kiniwa, Y.; Ashida, A.; Goto, Y.; Shang, W. H.; Kubodera, M.; Kato, M.; Takata, M.; Saida, T.; Kamata, T. NADPH oxidase 4 contributes to transformation phenotype of melanoma cells by regulating G2-M cell cycle progression. *Cancer research* **69:**2647-2654; 2009.

[36] Zhao, Y.; Liu, J.; McMartin, K. E. Inhibition of NADPH oxidase activity promotes differentiation of B16 melanoma cells. *Oncology reports* **19:**1225-1230; 2008.

[37] Lasaga, M.; Debeljuk, L.; Durand, D.; Scimonelli, T. N.; Caruso, C. Role of alpha-melanocyte stimulating hormone and melanocortin 4 receptor in brain inflammation. *Peptides* **29:**1825-1835; 2008.

[38] Bertolotto, C.; Abbe, P.; Hemesath, T. J.; Bille, K.; Fisher, D. E.; Ortonne, J. P.; Ballotti, R. Microphthalmia gene product as a signal transducer in cAMP-induced differentiation of melanocytes. *The Journal of cell biology* **142:**827-835; 1998.

FIGURE LEGENDS

Figure 1. Effect of systemic POMC overexpression on apoptosis in melanoma tissue. (A) The representative profiles of TUNEL staining in Ad-GFP- and Ad-POMC-treated melanoma. Apoptotic cells in melanoma were detected by TUNEL staining (green) while the cell nucleus was counter-stained with propidium iodide (PI; red). (B) Quantification of apoptotic index in Ad-POMC- and Ad-GFP-treated melanoma. The apoptotic index is expressed as a ratio of number of TUNEL positive cells over number of PI positive cells. Data are expressed as mean ± SEM from 6 experiments. (C) Correlation of apoptosis and hypoxia in in melanoma. Hypoxia activity and apoptosis in melanoma tissues was detected by hypoxyprobe-1 kit (pimonidazole; green) and TUNEL (red) assay respectively, followed by counterstaining with DAPI (blue). Arrows indicate hypoxic cells. Scale bar, 20 μm. *: $p < 0.05$.

Figure 2. Effect of POMC expression on sensitivity of melanoma cells to hypoxia. (A) Flow cytometry analysis of cells obtained from pre-G0 phase shows that Ad-POMC gene delivery increased apoptotic cells when compared to Ad-GFP group in hypoxia chamber. (B) Effect of hypoxia mimetic $CoCl_2$ on cell apoptosis. (C) POMC gene delivery triggered caspase 3 cascade activation in B16-F10 melanoma cells during hypoxia. The ratio of caspase-3 activity was measured by colorimetric caspase 3 activation assay. Data are expressed as means ± SEM from triplicate experiments. *: $p < 0.05$, **: $p < 0.01$.

Figure 3. The effect of POMC-derived peptides on sensitivity of melanoma cells to hypoxia. Representative flow cytometry demonstrating the effect of α-MSH, β-MSH, ACTH and γ-MSH neuropeptides (10 nM for each peptide) on cell population under normal and $CoCl_2$-induced hypoxic conditions. The percentage of apoptotic cells is expressed as mean ± SEM from triplicate experiments. **: $p < 0.01$.

Figure 4. Excess ROS production by POMC gene delivery triggered apoptotic process in B16-F10 melanoma cells during hypoxia. (A) The representative profiles of TUNEL and DHE co-staining in Ad-GFP- and Ad-POMC-treated melanoma. The apoptotic cells in melanoma were detected by TUNEL staining (green) while the cellular superoxide anion

(O2-) were indicated with DHE (red). The cells nucleic were counter-stained with DAPI (blue). Scale bar, 500 μm. (B) Measurement of intracellular ROS generation by DCF-DA staining. (C) The extracellular hydrogen peroxide (H_2O_2) production was measured by Amplex red assay. (D) Flow cytometry analysis shows that blocking ROS generation by N-acetyl-cysteine (NAC, 10 mM) could rescue Ad-POMC-induced apoptosis in hypoxia. (E) The ratio of caspase-3 activity was measured by colorimetric caspase 3 activation assay. Data are expressed as means ± SEM from triplicate experiments. *: $p < 0.05$, **: $p < 0.01$.

Figure 5. Effect of POMC-derived peptides on ROS generation and associated with an upregulation of Nox4 in hypoxia. (A, B) Clarification POMC-derived peptide α-MSH, β-MSH, ACTH and γ-MSH (10 nM) stimulated ROS generation capability by DCFH-DA and Amplex red assay. (C) The source of ROS generation. Analysis of ROS generation in the absence and presence of DPI (0.1 μM), allopurinol (50 μM) and indomethacin (1 μM) following α-MSH stimulation by Amplex red assay. (D and E) The effect of α-MSH on The Nox4 gene and protein expression in the absence or presence $CoCl_2$ (100 μM). Data are expressed as mean ± SEM from triplicate experiments. *: $p < 0.05$, **: $p < 0.01$.

Figure 6. Effect of Nox4 silencing on ROS generation and apoptosis in B16-F10 melanoma cells. Cells were transfected with control siRNA or Nox4 siRNA for 48 h before cell harvest. (A) Nox4 siRNA reduced the basal Nox4 mRNA and protein expression. (B) Nox4 siRNA remarkably impaired total ROS generation measured by Amplex red assay in the absence and presence $CoCl_2$ (100 μM). (C) Silencing Nox4 expression rescued α-MSH induced apoptosis $CoCl_2$ challenge compared to control siRNA group. Data are expressed as means± SEM from triplicate experiments. *: $p < 0.05$, **: $p < 0.01$. #: $p < 0.01$

Table 1

The effect of POMC-derived neuropeptides on the cell cycle of B16-F10 melanoma cells

		PreG0	G0/G1	S	G2/M
Normoxia	Control	0.14±0.33	57.00±2.81	18.24±0.24	24.81±3.35
	α-MSH	0.31±0.72	71.36±0.25*	8.54±0.89	19.88±1.29
	β-MSH	0.41±1.21	71.48±0.05*	8.62±0.45	19.55±1.54
	ACTH	0.28±1.05	71.78±1.53*	9.72±0.65	18.31±0.08
	γ-MSH	0.49±0.58	57.29±1.40	18.29±1.35	24.15±0.59
Hypoxia	Control	3.16±0.14	61.99±0.81	13.22±0.98	21.86±0.19
	α-MSH	10.85±3.19*	59.92±0.71	11.03±2.75	18.45±1.18
	β-MSH	10.11±1.16*	60.21±1.83	11.05±1.96	18.89±1.08
	ACTH	12.74±0.13*	59.65±0.45	11.19±2.17	16.65±1.83
	γ-MSH	3.74±0.05	59.19±2.30	12.83±1.48	24.41±0.72

*$p < 0.05$ versus Control.

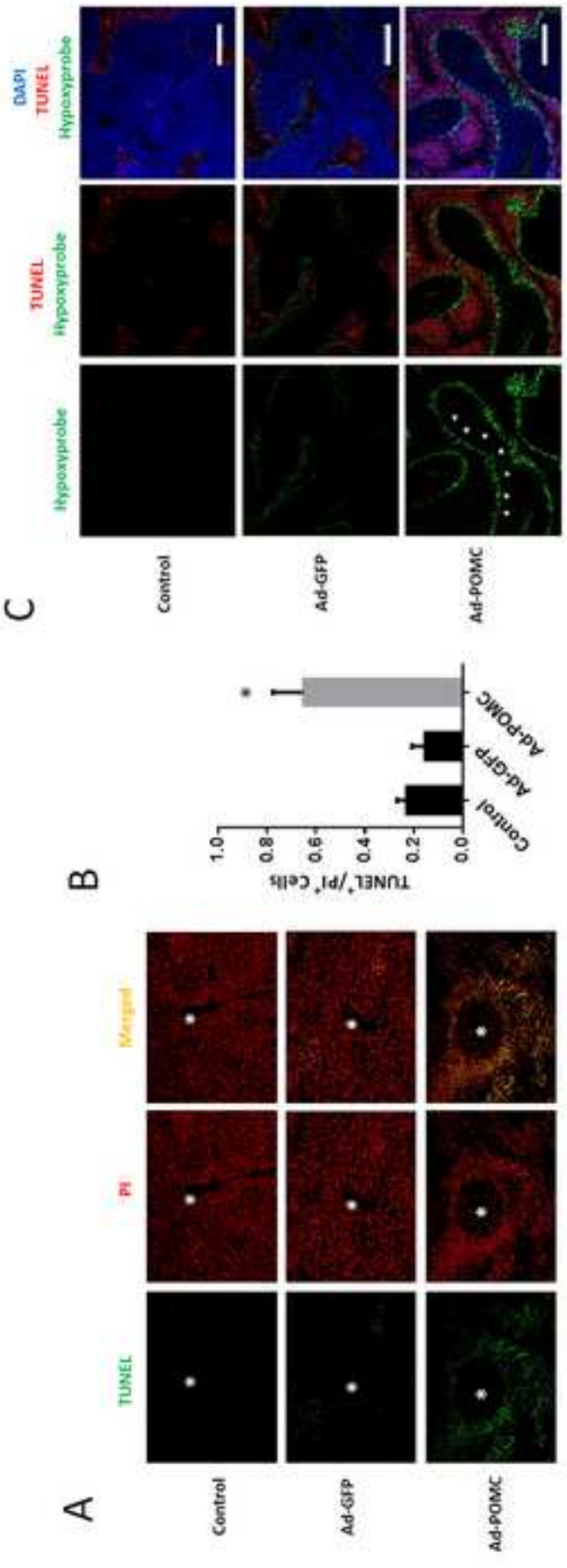

Figure 1

Figure 2

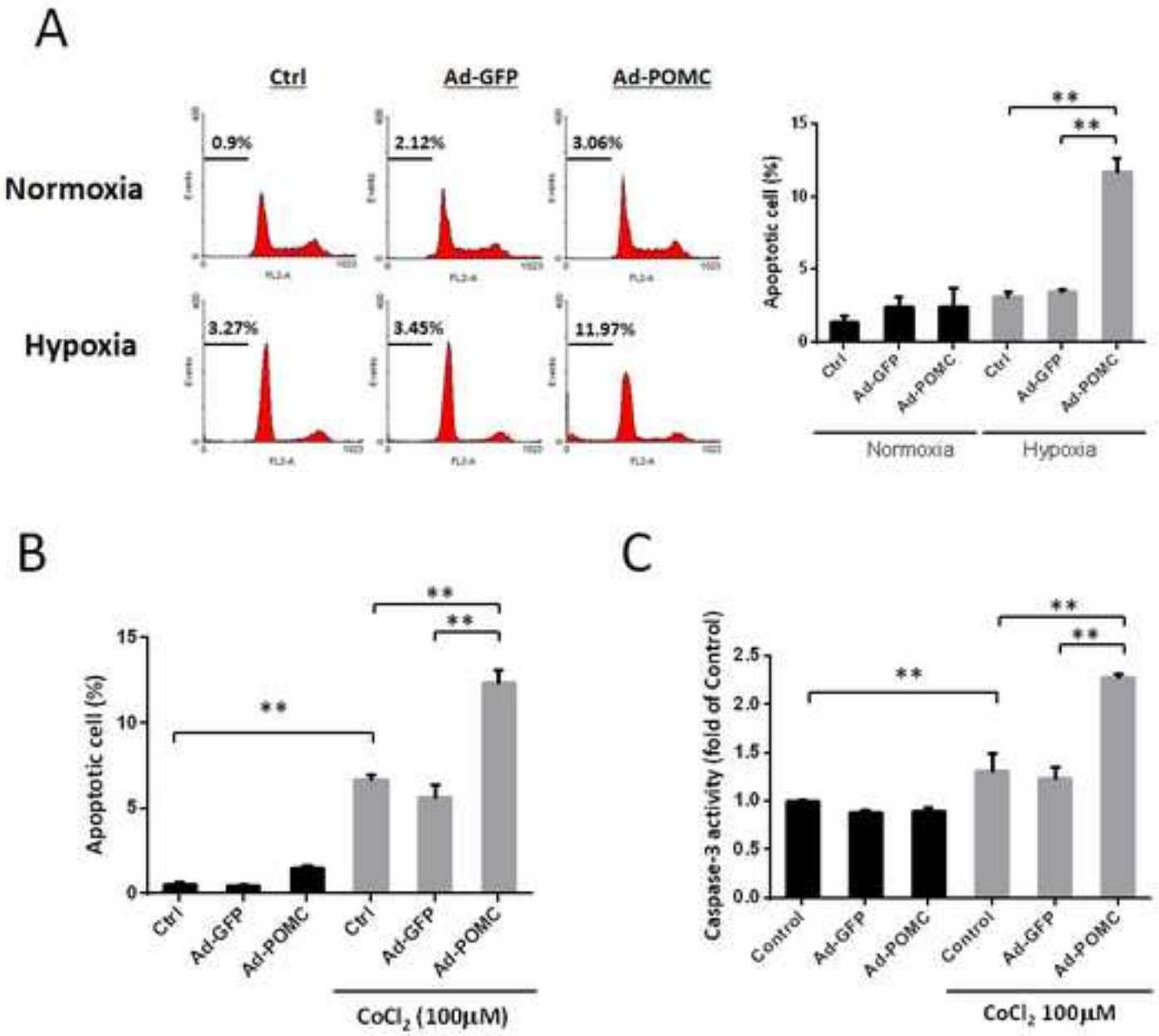

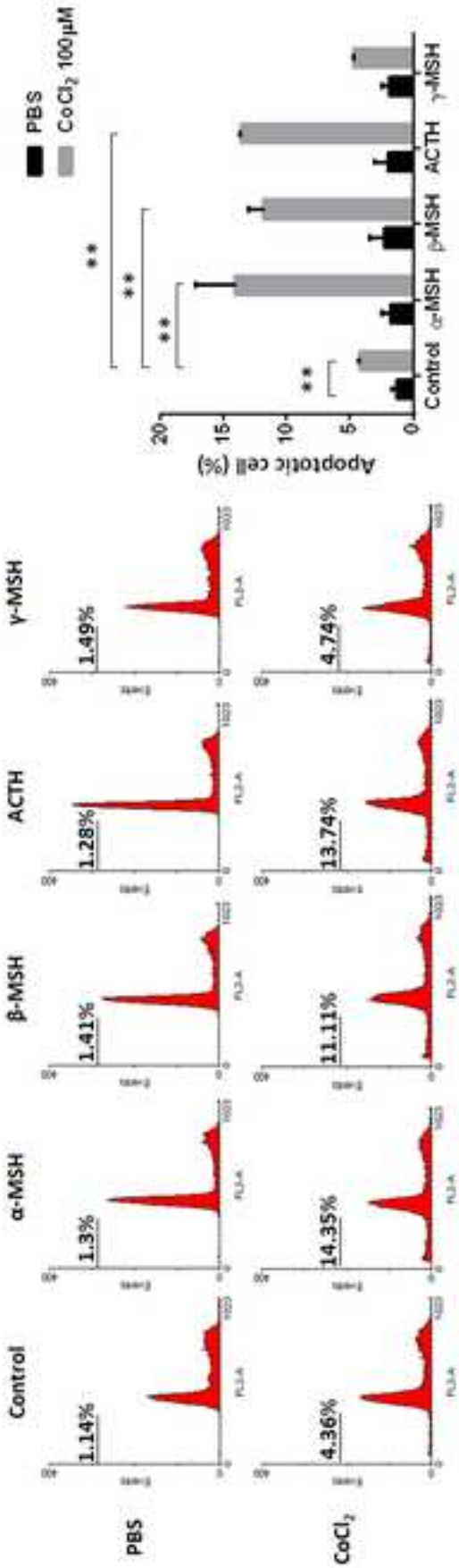

Figure 3

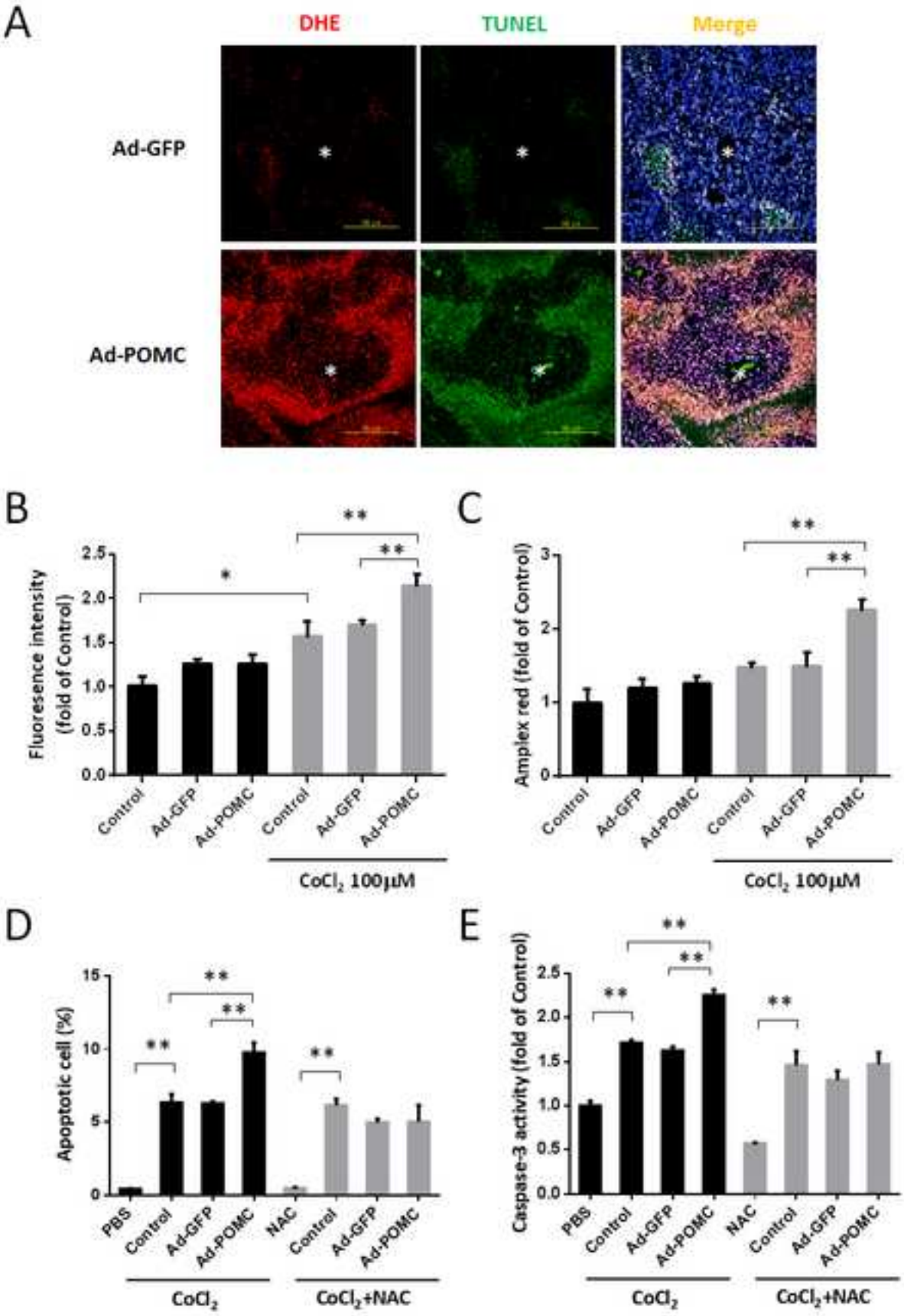

Figure 5

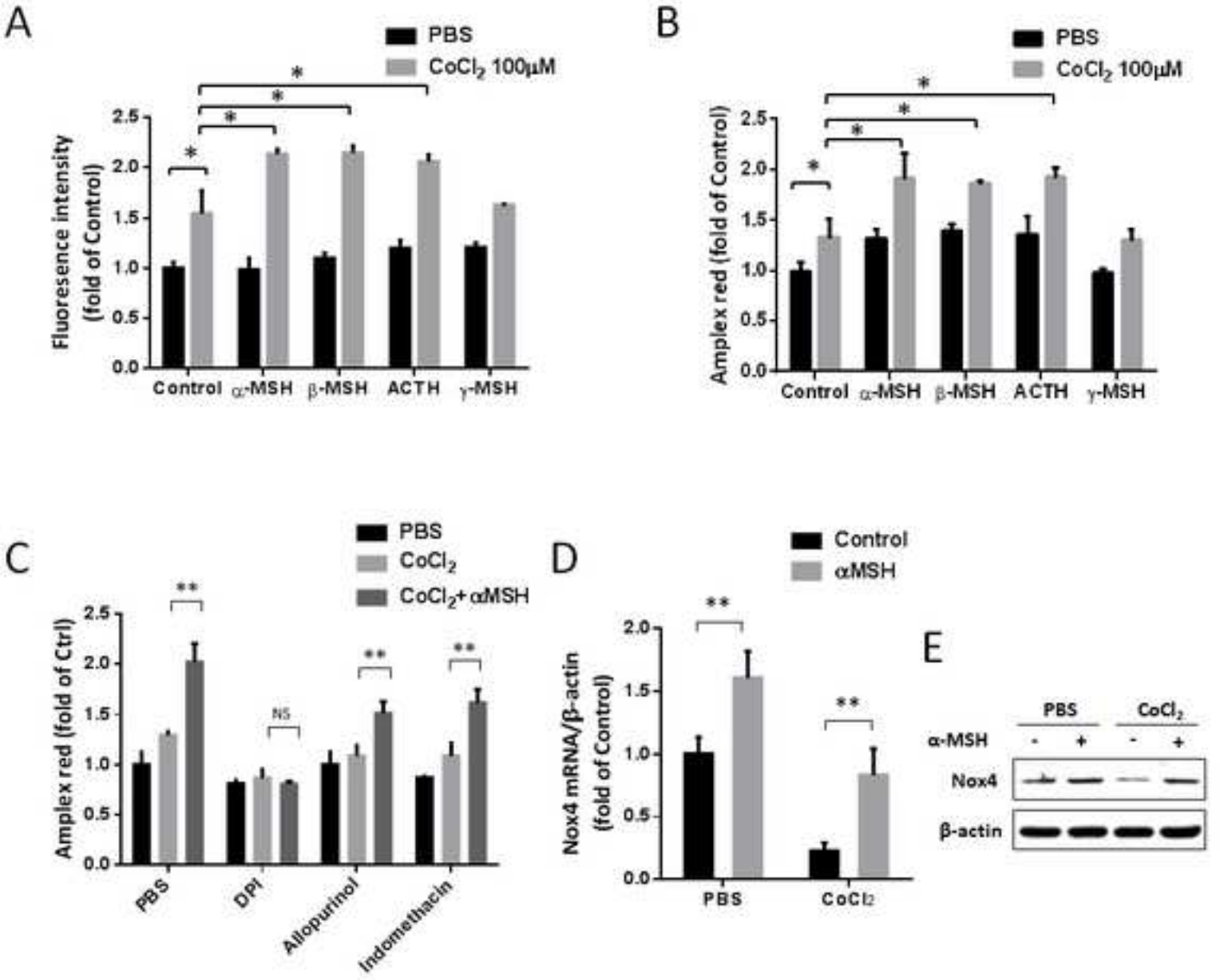

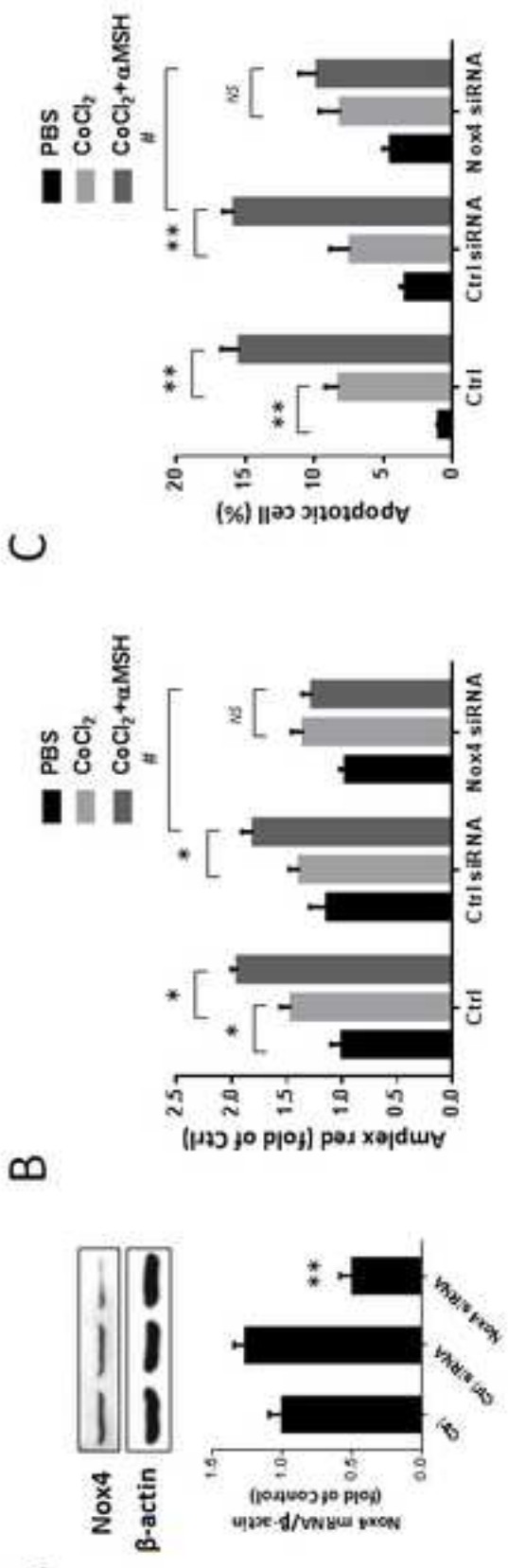
A
Nox4
β-actin
Nox4 mRNA/β-actin (fold of Control)
Ctrl
Ctrl siRNA
Nox4 siRNA
B
PBS
CoCl2
CoCl2+αMSH
Amplex red (fold of Ctrl)
Ctrl
Ctrl siRNA
Nox4 siRNA
C
PBS
CoCl2
CoCl2+αMSH
Apoptotic cell (%)
Ctrl
Ctrl siRNA
Nox4 siRNA

Figure 6